

# Estuaries are not so unique

David Prandle<sup>a</sup>, Andrew Lane<sup>a,\*</sup> and Andrew J. Manning<sup>b,c</sup>

<sup>a</sup> Proudman Oceanographic Laboratory, Joseph Proudman Building, 6 Brownlow Street, Liverpool L3 5DA, UK

<sup>b</sup> HR Wallingford Ltd, Estuaries & Dredging Group, Howbery Park, Wallingford, Oxfordshire OX10 8BA, UK

<sup>c</sup> Centre for Coastal Dynamics and Engineering, School of Earth, Ocean & Environmental Sciences, University of Plymouth, Portland Square Building, Plymouth PL4 8AA, UK

## Abstract

The applicability of recent theories relating tides and river flow to estuarine bathymetry has been assessed against observations from UK estuaries. These theories, combined with observations, show that the distinctiveness of estuaries is restricted by the way in which tides and river flow control sediments and bathymetry. The theories can explain the estuarine bathymetry without needing to account for the sediment dynamics, suggesting that it is the bathymetry which determines the sediment regime within the estuary. Typical ages were determined for Rias (11,000 years), Coastal Plain (15,000 years) and Bar-Built (100 years) estuaries.

*Keywords:* general oceanography, estuarine processes, data sets, Europe

## 1. Introduction

Estuaries serve diverse interests ranging from sustaining flora and fauna, navigation and recreation, to shore-based industrial and residential development. Long term management requires understanding of the relative vulnerability/sensitivity of specific estuaries. In particular, to accommodate impacts from Global Climate Change and localized ‘interventions’, we need forecasts of bathymetric evolution over future decades.

### 1.1. Uniqueness of estuaries

Estuaries are commonly defined as places where tidal action mixes waters from the sea and rivers, with accompanying claims that “each estuary is unique” (e.g., p4 in Dyer [1997]; *Estuarine Research Federation*, <http://erf.org/education/>). Here, we summarize new theories [Prandle, 2004a] that show how tides and river flows determine estuarine bathymetries. The range of validity of these theories has been subsequently assessed [Prandle, 2005] against a recently available data set [Burgess *et al.*, 2002]. We now apply these theories, alongside observational evidence, to show how the ‘uniqueness’ is constrained within bathymetric and sedimentary frameworks delineated by the controlling tides and river flows.

---

\* Corresponding author  
E-mail: [a.lane@pol.ac.uk](mailto:a.lane@pol.ac.uk) (A. Lane)

These new frameworks can readily be used for enhancing our understanding of existing morphologies and identifying anomalous estuaries. Where sediment deposition rates are much less than the (relative) rate of sea level rise, differences between observed and theoretical depths can be used for estimating the ‘age’ of estuaries. The frameworks can also be used for calculating future bathymetric evolution for prescribed changes in mean sea level, tidal amplitude, river flow, and sediment supply.

### 1.2. Ranges of estuarine parameters

While individual estuaries exhibit localized features (related to underlying geology, flora and fauna, historical development and ‘intervention’), conditions in most ‘mixed’ estuaries (requiring tidal elevation amplitude  $\zeta > 1$  m [Prandle, 2004a]) in temperate latitudes lie within the ranges given in Table 1.

This paper provides theoretical and observational background and perspective for understanding the dynamics and morphology of an estuary and its likely sensitivity to change.

## 2. Theory

Equations for the tidal elevation, currents, tidal intrusion length and depth at the mouth, are combined with conditions for saline and tidal intrusion, stratification, and additionally the estuarine parameter ranges (Table 1) to establish the extent of viable estuarine characteristics.

### 2.1. Tidal elevations and currents

The axial ( $x$ ) momentum equation for tidal propagation can be approximated by

$$\frac{\partial u}{\partial t} + g \frac{\partial Z}{\partial x} + \frac{fu|u|}{D} = 0, \quad (1)$$

where  $u$  is the tidal velocity,  $Z$  is the elevation,  $D$  is depth, and  $f$  is the bed friction coefficient. Harmonic solutions for the predominant tidal constituent take the form:  $Z = \zeta \exp\{i(-\omega t + kx)\}$  and  $u = U \exp\{i(-\omega t + \theta + kx)\}$ . By assuming the surface slope is due to axial variation in tidal phase (rather than amplitude) and substituting for  $Z$  and  $u$ , Equation (1) becomes:

$$U\{1 + i 1.33fU/(\omega D)\} \exp(i\theta) = \zeta(g/D)^{1/2}, \quad (2)$$

where the phase celerity  $\omega/k$  is assumed to be  $(gD)^{1/2}$  and the linearization of the quadratic friction term follows from *Prandle* [2004a]. Assuming  $M_2$  is the predominant tidal constituent, (2) can provide quantitative insight into the relevant importance of the (first) inertial versus (second) friction terms in balancing the surface gradient forcing:

$$U(1 + i23.7U/D) \exp(i\theta) = 3.1 \zeta D^{1/2}. \quad (3)$$

Noting the parameter range indicated in Table 1, it is evident that in waters of less than 10 m, friction will dominate and a simple expression for tidal current amplitude follows:  $U = 0.36 \zeta^{1/2} D^{1/4}$ . This explains the restricted range of tidal currents in estuaries, with values almost invariably in the range 0.5 to 1.0 m s<sup>-1</sup> as indicated in Figure 2, based on a complete solution to (1).

Despite the immense range of shapes and sizes of Shelf Seas and their coastal fringes, there are few sites where the mean amplitude of ocean tides exceeds 4 m. With intertidal slopes of typically 0.001, the water interface advances at up to  $0.14 \times \zeta$  m s<sup>-1</sup> over intertidal areas  $2 \times \zeta$  km wide. It might be expected that with extreme values of  $\zeta$ , these conditions would lead to wide-scale morphological adjustments in a manner that effectively reduces further tidal amplification.

## 2.2. Bathymetric theories

By assuming a ‘synchronous’ estuary, where surface gradients generated by tidal phase change predominate over those via tidal amplitude variations, *Prandle* [2004a] derived the following expression for the length of tidal intrusion in an estuary

$$L = 123 D^{5/4} / (\zeta f)^{1/2} = 2460 D^{5/4} / \zeta^{1/2} \quad (\text{m}), \quad (4)$$

where  $D$  is depth (m),  $\zeta$  tidal elevation amplitude (m) and  $f$ , the bed friction coefficient is taken as 0.0025. *Prandle* [2004a] deduced from observations that mixing of river and salt water occurs as seawards as possible, subject to being contained within the estuary. Using Equation (9) for the length of saline intrusion,  $L_i$ , the following expression is obtained:

$$D = 12.8 (Qa)^{0.4}, \quad (5)$$

where  $a$  is the lateral slope of an assumed triangular cross section. This result is independent of both  $\zeta$  and  $f$ .

*Prandle* [2004a] determined a ‘zone of morphological existence’ bounded by the requirements that saline intrusion, and its associated tidal excursion, do not extend beyond the estuary:

$$\text{Tidal excursion: tidal length} \quad E_X/L < 1, \quad (6)$$

$$\text{Saline intrusion: tidal length} \quad L_1/L < 1. \quad (7)$$

An additional condition, limiting applications to ‘mixed’ estuaries, is the criterion of *Simpson and Hunter* [1974]

$$D/U^3 < 50 \text{ (m}^{-2} \text{ s}^3\text{)}. \quad (8)$$

Hence the basic estuarine dimensions of depth and length can be directly estimated from the two fundamental ‘forcing’ parameters namely tide and river flow. Moreover, since these parameters are also the most readily available data for many estuaries, wide-scale assessment of the theories is possible.

### 3. Data: range of estuaries

Figure 2 shows this ‘Morphological Zone’ together with observed data from the 96 UK estuaries shown in Figure 1. These estuaries are sub-divided into the major estuarine types of Ria, Coastal Plain, and Bar-Built [*Davidson and Buck*, 1997]. In general, Rias are short, deep, and steep-sided with small river flows. Coastal Plains are long and funnel-shaped with gently sloping triangular cross-sections providing extensive intertidal zones. Bar-built estuaries are short and shallow with small river flows and tidal range. Short estuaries tend to be sandy whereas long estuaries are muddy. In sedimentary terms, Bar-built estuaries are located along coasts with plentiful supplies of marine sediments and consequently, are closer to present-day equilibrium. Coastal Plain estuaries are continuing to infill following ‘over-deepening’ via post-glacial river flows, while Rias are drowned river valleys (with related cross-sections) as a consequence of (relative) sea level rise.

The theories were shown [*Prandle*, 2005] to be most directly applicable to Coastal Plain and Bar-Built estuaries, reflecting their geomorphological modes of generation and their relative independence from control by ‘hard geology’. Hence, we subsequently concentrate on these morphological types.

A systematic procedure for calculating representative depths from the original ‘Future-Coast’ [*Burgess et al.*, 2002] data set was used, namely  $D = 0.5 (V_H/S_H + V_L/S_L)$  where  $V$  is the net

volume, and  $S$  is the net surface area at High Water (H) and Low Water (L). The only estuaries excluded within the three types considered were those where the lengths were less than 2.5 km or no river flow data was available.

The distribution of estuaries is predominantly within the anticipated Morphological Zone – with a few ‘anomalies’ justifying further investigation. As expected, we note that, Coastal Plain estuaries are generally associated with larger tides and river flows. Strong tidal currents, almost invariably greater than  $0.5 \text{ m s}^{-1}$ , exclude (permanent) stratification in all of the estuaries considered.

### 3. Results

Estuaries in England and Wales are mapped onto a morphology chart according to river flow and tidal elevation amplitude data; Figures 2, 3 and 4, each represent different aspects of estuarine properties. Equations (6), (7) and (8) indicate the boundaries of the Morphological Zone in Figure 2, and contours for tidal velocity amplitudes  $0.5$  and  $1.0 \text{ m s}^{-1}$  are also plotted. Figure 3 shows the distribution of estuarine lengths and depths identified in Figure 2. Superposed are theoretical loci for values of  $L = 5, 10$  and  $20 \text{ km}$ , based on Equations (4) and (5). The top axis shows the theoretical depths from (5) assuming the mean observed value of  $a = 0.013$ . Figure 4 indicates the sediment regime and flushing times, with additional sediment fall velocity and concentration data observed in several European estuaries [Manning, 2004].

### 4. Discussion

#### 4.1. River flow, $Q$

The question of the minimum flow necessary to maintain an estuary can be addressed by specifying that  $D > \zeta$ . Hence for  $\zeta = 1 \text{ m}$  and  $a = 0.01$ , Equation (5) gives  $Q = 0.17 \text{ m}^3 \text{ s}^{-1}$ , or  $Q = 1.7 \text{ m}^3 \text{ s}^{-1}$  for  $a = 0.001$ . These values of  $Q$  are increased by factors of 16 for  $\zeta = 3 \text{ m}$ . A minimum value of  $Q = 0.25 \text{ m}^3 \text{ s}^{-1}$  was found to be necessary to maintain tidal creeks [I. H. Townend, personal communication]. From (4), the estuarine length for  $D = \zeta = 1 \text{ m}$  is  $2.5 \text{ km}$ .

A representative maximum flow can be determined from the boundaries of the Morphological Zone (Figure 2) using the equivalent depth scale shown in Figure 3. This suggests that, in general,  $D < 20 \text{ m}$ , indicating  $Q < 3000 \text{ m}^3 \text{ s}^{-1}$  for a lateral slope of  $0.001$ . The theory suggests that for estuaries with greater flows  $L_1 > L$ , offshore plumes might be anticipated. Schubel and Hirschberg [1982] reported that only ten estuaries in the world have  $Q > 15,000 \text{ m}^3 \text{ s}^{-1}$ , thus the range indicated encompasses most estuaries. From (3) a maximum value of  $D = 20 \text{ m}$  corresponds to a maximum tidal intrusion length of  $100 \text{ km}$  for  $\zeta = 1 \text{ m}$ .

*Prandle* [2004b] showed that in ‘mixed’ estuaries (as considered here), the length of saline intrusion is given by

$$L_1 = 0.005 D^2 / (f U U_0), \quad (9)$$

where  $U_0$  is the residual velocity associated with river flow. Substituting (co-existing) minimum and maximum values for  $L$ ,  $D$  and  $U$  from Table 1, and requiring  $0.5 < L_1/L < 1$ , we obtain values of  $0.4 < U_0 < 1.3 \text{ cm s}^{-1}$ . Observational data, within the saline intrusion zone, from wide ranging sources generally substantiate this.

#### 4.2. Lengths and depths

Figure 3 shows the distribution of estuarine lengths and depths; the general trend for longer tidal reaches with larger flows is evident. Overall the observed values of depths and lengths are broadly consistent with the new dynamical theories. The small depths in Bar-Built estuaries are clearly demonstrated. By identifying Coastal Plain estuaries where depths diverge significantly from the theoretical background, estimates can be made of the much larger flows existent in their post-glaciation formation. The divergence can also be used for inferring coastal regions with scarcity of sediment supplies for infilling.

An estimate of the effect of changes in mean sea level (msl) on these estuaries was made by least squares fitting of the expression  $D_T(n) = D_O(n) - NS(n)$ , relating theoretical (subscript T), and observed (subscript O) depths.  $S(n)$  is the estimate, for each estuary, of the annual rate of relative sea level rise (extracted from *Shennan* [1989]). For Rias, a value of  $N \sim 11,000$  years was calculated, with the msl term increasing the percentage of variance accounted for (PVA) from 9% to 61%. Corresponding values for Coastal Plain estuaries were  $N \sim 15,000$  years increasing the PVA from 37% to 65% while for Bar-Built estuaries,  $N \sim 100$  years with negligible impact on the PVA of 64%. These results confirm the morphological theories of the development of estuarine bathymetries. The msl trends vary from  $-5$  to  $2.0$  mm per year; over 10,000 years, these amount to changes of  $-5$  to  $20$  m in estuarine depths.

#### 4.3. Sediment regimes and flushing times

Figure 4 shows loci of representative flushing times for river-borne dissolved or suspended sediments at 2 and 10 days based on the expression [*Prandle*, 2004a]:

$$t_F = 0.5 (L_1/2) / U_0, \quad (10)$$

with residual current  $U_0 = 1 \text{ cm s}^{-1}$ . Flushing times greater than the principal semi-diurnal tidal period provide valuable longer-term persistence of marine-derived nutrients, while flushing times less than the 15-day spring-neap cycle yield effective flushing of contaminants. Hence, there might be some ecological advantage to the bathymetric envelope defined by these two flushing times.

*Prandle* [2004a] derived an expression for depth and time-mean concentrations of fine suspended sediment (in  $\text{kg m}^{-3}$  equivalent to  $10^3 \text{ mg l}^{-1}$ ):

$$C = 5 \gamma \rho U, \quad (11)$$

where the erosion constant  $\gamma = 0.0001 \text{ m}^{-1} \text{ s}$ , and  $\rho$  is the water density ( $\text{kg m}^{-3}$ ). Corresponding loci for 250 and 500  $\text{mg l}^{-1}$  are shown in Figure 4, which assumes unlimited supply. (Note these curves correspond exactly to those for  $U = 0.5$  and  $1.0 \text{ m s}^{-1}$  in Figure 2.) These results illustrate why many estuaries show high levels of fine suspended sediments.

The above theories for estuarine bathymetry take no account of sediment dynamics. Their relative success provokes a reversal of the customary assumption that estuarine bathymetries are determined by their prevailing sediment regimes. *Prandle* [2004c] showed that the fall velocity of sediment types consistent with bathymetric equilibrium, i.e., yielding no net erosion or accretion, was

$$w_s = 0.61 f U. \quad (12)$$

From the restricted range for  $U$  discussed previously, (12) indicates a narrow range of fall velocities, typically between 1 and 3  $\text{mm s}^{-1}$  – corresponding loci for these fall velocities are shown in Figure 4.

*Manning* [2004] investigated settlement of fine sediments in a wide range of European estuaries, and found that settling was primarily via the formation of micro and macro-flocs, invariably close to the range suggested by the theory (12) above; his results are superposed in Figure 4. Likewise, prevailing observed suspended sediment concentrations are in good agreement with theoretical values from (11).

## 5. Conclusions

Even with the seemingly wide diversity in estuaries, the combined control of tides and river flows on their bathymetries and sediment regimes is shown – both from observations and new theories. Thus, for estuaries where salt and fresh water are mixed internally, representative minimum and maximum values can be prescribed for tidal currents, river flows (and attendant residual velocities), depths, lengths, flushing times, suspended sediment concentrations and fall velocities.

Close agreement between observed and theoretical values of suspended sediment concentration and fall velocities substantiates the paradigm reversal that sediment regimes are a consequence of the bathymetry – not the reverse as widely assumed. Using recently available data for 96 UK estuaries and by relating the difference between observed and theoretical depths to the years of (relative) sea level change since the estuary was formed, typical ages for Rias, Coastal Plain and Bar-built estuaries were calculated.

## Acknowledgment

This study was supported by Research Project FD2107 ‘Development of Morphological Models’. The Project forms Part 2 of the UK Estuaries Research Programme funded by the ‘Broad Scale Modelling Theme’ within Defra/Environment Agency’s Flood Management Research Programme.

## References

- Burgess, K. A., P. Balson, K. R. Dyer, J. Orford and I. H. Townend (2002), Future-Coast – the integration of knowledge to assess future coastal evolution at a national scale, in *28th International Conference on Coastal Engineering*, 3, pp3221–3233, ASCE, New York.
- Davidson, N. C. and A. L. Buck (1997), *An Inventory of UK Estuaries, Vol. 1* (of 7), ‘Introduction and Methodology’ published by Joint Nature Conservation Council, UK. ISBN 1 873701 36 5.
- Dyer, K. R. (1997) *Estuaries: A Physical Introduction*, 2nd edition, 195pp, Wiley, Chichester. ISBN 0 41 97471 4.
- Manning, A. J. (2004), Observations of the properties of flocculated cohesive sediment in three western European estuaries, in *Sediment Transport in European Estuaries*, edited by P. Ciavola and M. B. Collins, pp70–81, *Journal of Coastal Research*, SI 41.
- Prandle, D. (2004a), How tides and river flows determine estuarine bathymetries, *Progress in Oceanography*, 61, 1–26, doi:10.1016/j.pocean.2004.03.001.
- Prandle, D. (2004b), Saline intrusion in partially mixed estuaries, *Estuarine, Coastal and Shelf Sciences*, 59(3), 385–397, doi:10.1016/j.ecss.2003.10.001.
- Prandle, D. (2004c), Sediment trapping, turbidity maxima and bathymetric stability in macro-tidal estuaries, *Journal of Geophysical Research*, 109, C08001–13, doi:10.1029/2004JC002271.
- Prandle, D. (2005), Dynamical controls on estuarine bathymetry: assessment against UK data base, submitted to *Estuarine, Coastal and Shelf Sciences*.
- Schubel, J. R. and D. J. Hirschberg (1982), The Chang Jiang (Yangtze) Estuary: Establishing its place in the community of estuaries, in *Estuarine Comparisons*, edited by V. S. Kennedy, pp649–54, Academic Press, New York.
- Shennan, I. (1989), Holocene crustal movements and sea-level changes in Great Britain, *Journal of Quaternary Science*, 4(1), 77–89.
- Simpson, J. H. and J. R. Hunter (1974), Fronts in the Irish Sea, *Nature*, 250, 404–406.

Table 1  
Conditions in ‘mixed’ estuaries at temperate latitudes.

	Range	Units
<i>Tidal forcing, saline intrusion</i>		
Tidal elevation amplitude	$1^* < \zeta < 4$	m
Tidal current amplitude	$0.5 < U < 1.25$	$\text{m s}^{-1}$
River flow	$0.25 < Q^\dagger < 3000^\ddagger$	$\text{m}^3 \text{s}^{-1}$
Associated current	$0.001 < U_0^\S < 0.01$	$\text{m s}^{-1}$
Flushing time	$1 < t_F < 15$	days
<i>Bathymetry</i>		
Depth at the mouth	$1^{**} < D < 20^\ddagger$	m
Tidal intrusion length	$2.5^{**} < L < 100^\ddagger$	km
Age	$100 < Y < 15000$	years
<i>Sediment regime</i>		
Suspended concentration	$200 < C^{\dagger\dagger} < 750$	$\text{mg l}^{-1}$
Fall velocity	$0.5 < w_s^{\ddagger\dagger} < 5$	$\text{mm s}^{-1}$

\* for ‘mixed’ estuaries

† implications for spacing between estuaries

‡ for mixing within the estuary

§ in the saline intrusion zone

\*\* for continuous functioning over the tidal cycle

†† assuming ‘unlimited supply’

‡‡ via floccs

## List of Figures

Fig. 1. Locations and morphological types of the 96 Future-Coast estuaries [*Burgess et al.*, 2002].

Fig. 2. Morphological Zone, ( $\zeta$ ,  $Q$ ) coordinates of estuaries.

Continuous lines show  $E_x/L = 1$ ,  $L_1/L = 1$  and  $D/U^3 = 50 \text{ m}^{-2} \text{ s}^3$ .

$E_x$  is the tidal excursion,  $L_1$  is salinity intrusion, and  $D/U^3$  criterion of *Simpson and Hunter* [1974].

Dashed contours for tidal velocity amplitude  $U = 0.5$  and  $1.0 \text{ m s}^{-1}$ .

Dotted line shows Simpson-Hunter stratification demarcation.

Fig. 3. Estuarine lengths and depths.

Digits show observed values; left – depths (m), right – **lengths** (km).

Contours show theoretical values (Equation 3) for  $L = 5, 10$  and  $20$  km.

Top axis shows depths from (5) for lateral slope,  $a = 0.013$ .

Fig. 4. Sedimentary regime and flushing times.

Dotted contours show flushing times (Equation 10) of 2 and 10 days.

Dashed contours show time- and depth-averaged suspended sediment concentrations (11) for 250 and  $500 \text{ mg l}^{-1}$ .

Continuous contours correspond to bathymetric equilibrium for fall velocities (12) of 1 and  $3 \text{ mm s}^{-1}$ .

Observed fall velocities (left) and **concentrations** (right) on ● spring and ○ neap tides [*Manning, 2004*] in the Tamar, Schelde, Gironde, etc.

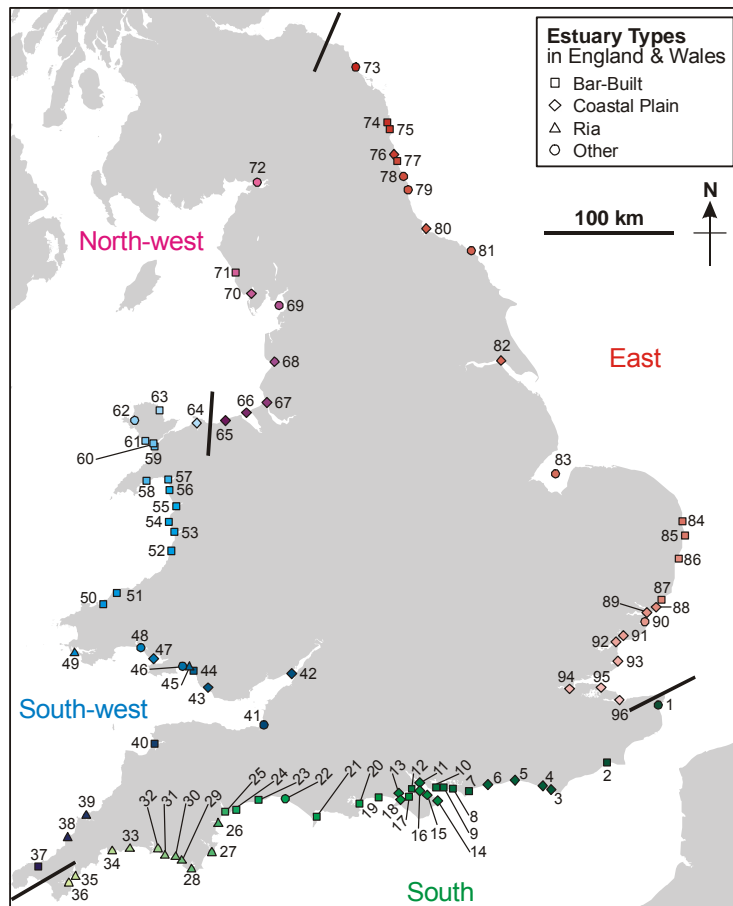


Fig. 1. Locations and morphological types of the 96 Future-Coast estuaries [Burgess *et al.*, 2002].

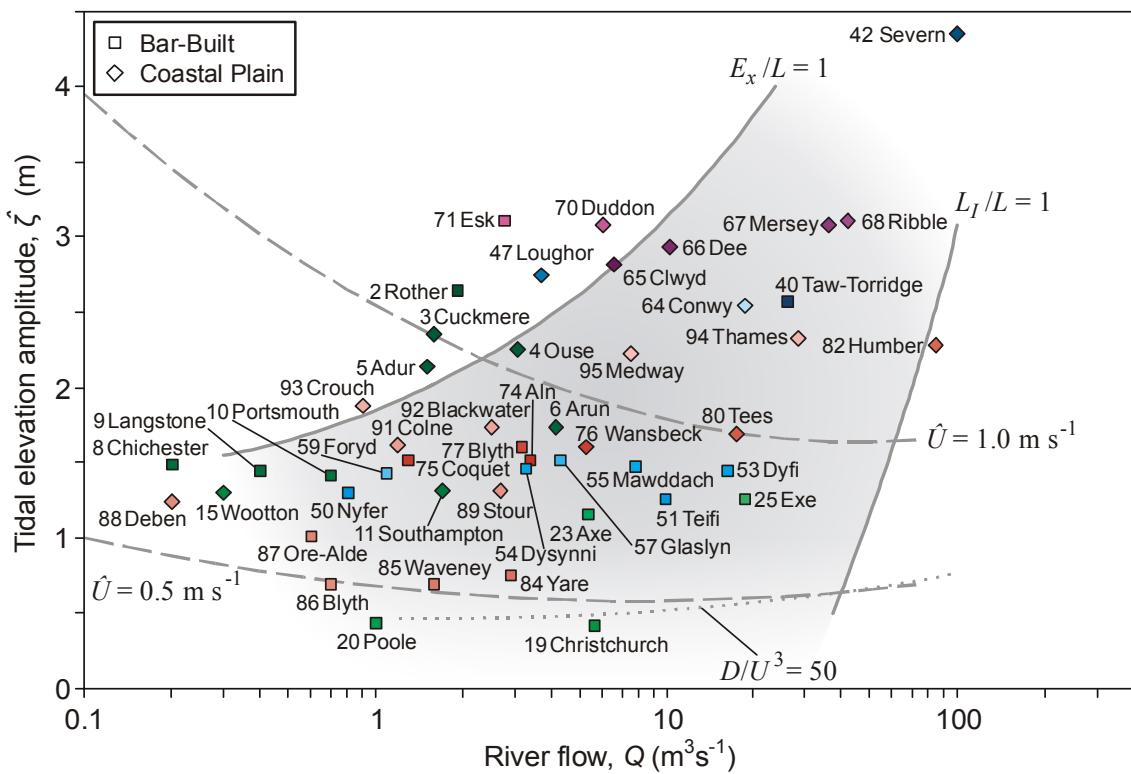


Fig. 2. Morphological Zone,  $(\zeta, Q)$  coordinates of estuaries. Continuous lines show  $E_x/L = 1$ ,  $L_I/L = 1$  and  $D/U^3 = 50 \text{ m}^{-2} \text{ s}^3$ .  $E_x$  is the tidal excursion,  $L_I$  is salinity intrusion, and  $D/U^3$  criterion of *Simpson and Hunter* [1974]. Dashed contours for tidal velocity amplitude  $U = 0.5$  and  $1.0 \text{ m s}^{-1}$ . Dotted line shows *Simpson-Hunter* stratification demarcation.

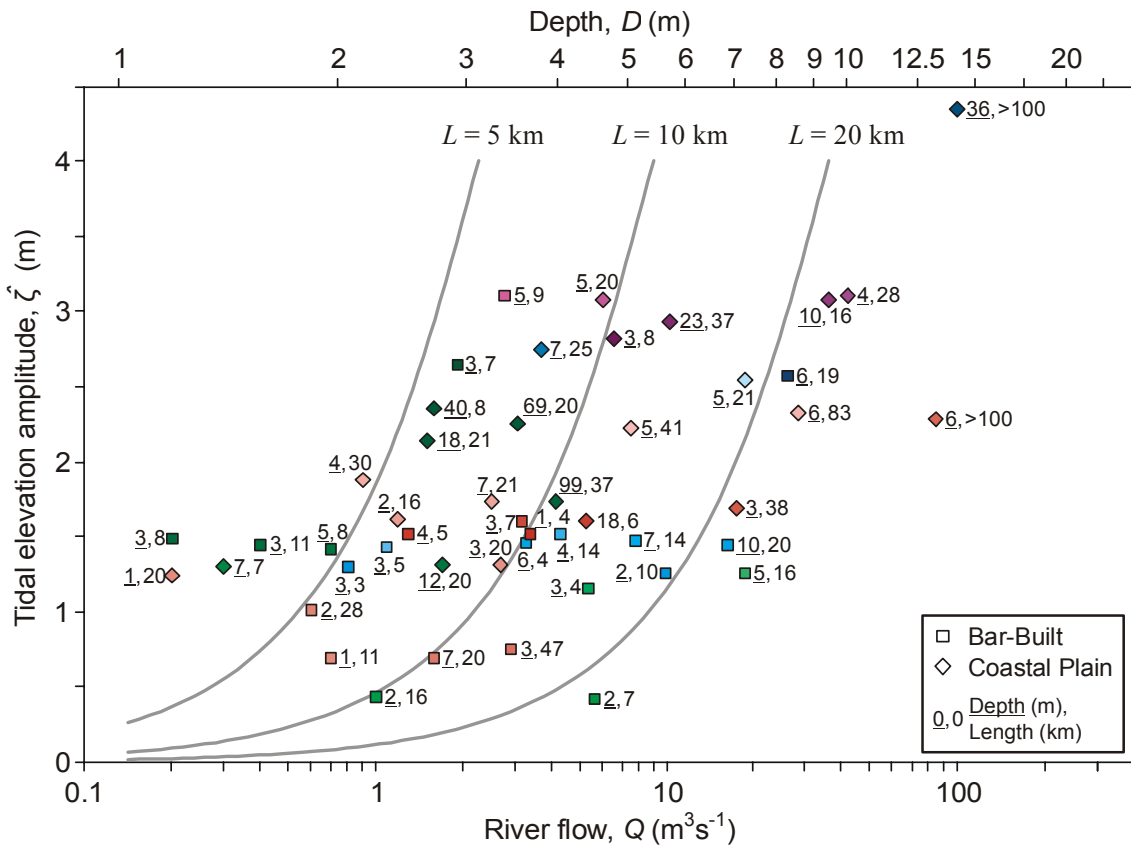


Fig. 3. Estuarine lengths and depths. Digits show observed values; left – depths (m), right – lengths (km). Contours show theoretical values (Equation 3) for  $L = 5, 10$  and  $20$  km. Top axis shows depths from (5) for lateral slope,  $a = 0.013$ .

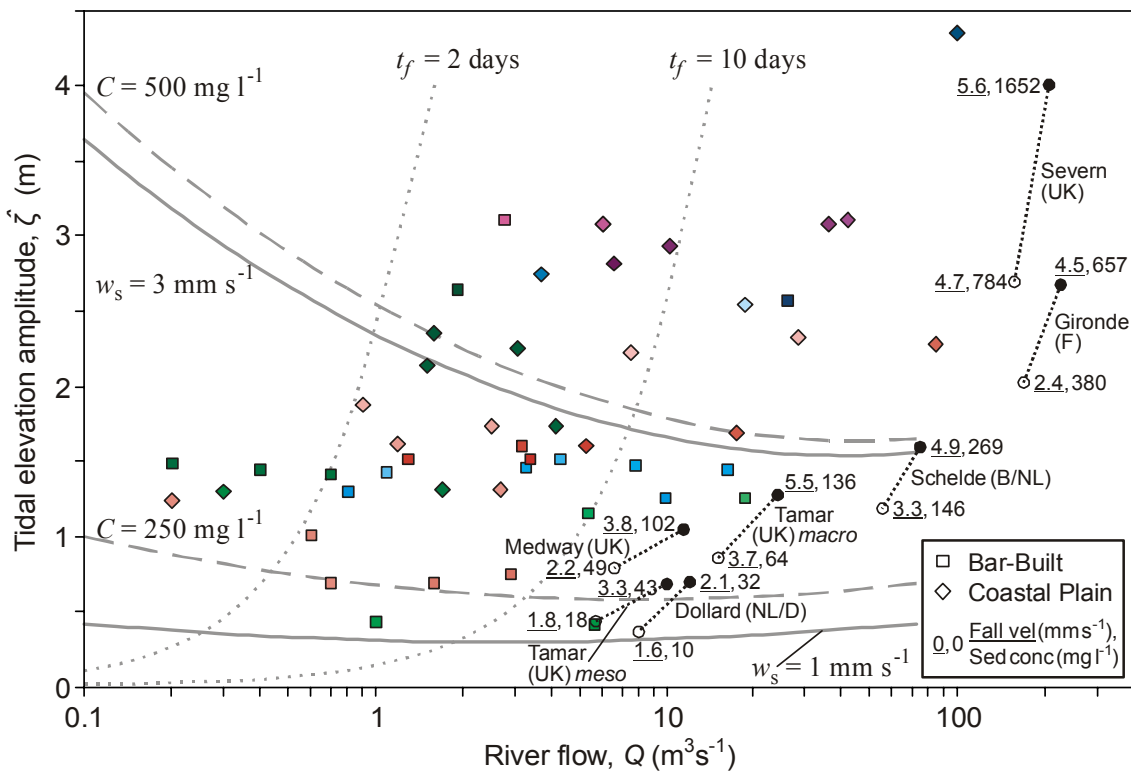


Fig. 4. Sedimentary regime and flushing times. Dotted contours show flushing times (Equation 10) of 2 and 10 days. Dashed contours show time- and depth-averaged suspended sediment concentrations (11) for  $250$  and  $500$   $\text{mg l}^{-1}$ . Continuous contours correspond to bathymetric equilibrium for fall velocities (12) of  $1$  and  $3$   $\text{mm s}^{-1}$ . Observed fall velocities (left) and concentrations (right) on  $\bullet$  spring and  $\circ$  neap tides [Manning, 2004] in the Tamar, Schelde, Gironde, etc.